NASA Technical Memorandum 88855

IN-27198

Ultrasonic Determination of Recrystallization

Edward R. Generazio
Lewis Research Center
Cleveland, Ohio

Prepared for
Review of Progress in Quantitive NDE
cosponsored by Ames Laboratory and Iowa State University
La Jolla, California, August 3-8, 1986

NASA

ULTRASONIC DETERMINATION OF RECRYSTALLIZATION

Edward R. Generazio

National Aeronautics and Space Administration
Lewis Research Center
Cleveland, OH.

E-3248

INTRODUCTION

Metals are currently used in a wide variety of applications ranging from simple structural to complex heat engine components. Each use has a different set of engineering characteristics that must be met by the material being considered for use. One method to tailor material properties to meet engineering requirements is thermomechanical processing (TMP).[1,2] If TMP involves cold working, metals generally show a marked increase in strength, but this increase does not continue without limit as the microstructure becomes distorted and exhibits high internal stress. These residual stresses are generally detrimental to the end use applications.

Further modification of the material can be obtained by annealing the material at various intervals during the cold working process. Annealing serves two main purposes. (1) To relax residual stresses and (2) to recrystallize (soften) the material. Stress relieving results in partial softening due to the movement and annihilation of dislocations[3,4] while recrystallization yields a total softening by the complete replacement of the worked microstructure with an essentially dislocation free new grain structure. Both of these processes are dependent on the amount of prior cold work, temperature, and time where the time to complete the process decreases as the amount of work or temperature increases.

In the case of recrystallization there are several experimentally measurable material properties that exhibit marked variations. Four of the most common material characteristics[1-3] are hardness, strength, ductility, and microstructural changes. The experimental signatures of each of these after recrystallization are (1) the material hardness decreases, (2) the yield strength decreases, (3) the ductility increases, and (4) a free grain structure appears. While these changes can be observed by mechanically testing, and metallographic, diffractive x-ray and transmission electron microscopic examination, generally destructive testing methods are required.

It is shown here that the nondestructive measurement of ultrasonic attenuation can identify and characterize the state of the recrystallization. The interrelation between ultrasonic attenuation and recrystallization thermal kinetics yields a technique for determining onset, degree, and completion of recrystallization.

THEORY

We are concerned here with the ultrasonic interaction with material microstructure and the thermal process of recrystallization. Two theories covering acoustic-microstructure[5-7] interaction and the thermal kinetics of recrystallization[8-10] need to be examined. It is assumed that the acoustic interaction with the microstructure is dominated by grain scattering[6] and/or dislocation damping.[7] Other acoustic-microstructural interactions leading to magnetoelastic and thermoelastic effects[5] are not expected to change substantially and/or concurrently with recrystallization.

The attenuation a_g due to grain scattering is given by[6]

$$a_r = C_r D^3 F^4 \text{(Rayleigh)} \quad \text{and} \quad a_s = C_s D F^2 \text{ (Stochastic)} \tag{1}$$

where the C's are constants dependent on density, velocity, etc., D is the mean grain diameter, F is frequency. When the wavelength of sound is much greater than the mean grain diameter or scatterer size, we have Rayleigh scattering with a fourth power frequency dependence. When the scatterer size is on the order of the sound wavelength we have stochastic scattering with a second power frequency dependence. Equation (1) should not be expected to apply to an arbitrary metal consisting of a size distribution of topologically complex grains. However, we may identify the frequency exponent as a key variable. That is, if grains are growing from small (Rayleigh) to large (stochastic) scatterers is is expected that the frequency exponent, over a fixed frequency range, should decrease with increasing grain size.

The attenuation due to dislocation damping a_d is given by[7]

$$a_d = gCW(F,F_0) \tag{2}$$

where g is the dislocation density, C is a constant dependent on shear modulus, dislocation damping force, etc., and W is a complicated function of the resonant frequency F_0. Equation (2) applies to materials containing a dilute noninteracting collection of dislocation lines oriented normal to the sound direction. Equation (2) does not apply to the intertwined network of dislocations observed in mechanically worked materials. Equation (2) does, however, imply that if dislocation damping is dominant attenuation mechanism then a decrease in dislocation density should result in a corresponding decrease in attenuation.

THERMAL KINETICS

Mechanically working a metal produces a dense collection of germ nuclei within the material. These germ nuclei, when activated by an increase in temperature, transform (i.e., recrystallize) into small crystallites which subsequently grow into fully developed grains. The transformed volume is given by[8-10]

$$\frac{V_R}{V} = \sum_{i=1}^{M} \left\{ 1 - \exp\left[-SG^3 N_0 t^3 \exp\left(-\frac{U}{RT_i} \right) \right] \right\} \tag{3}$$

where V_R is the volume that has recrystallized and V is the initial unrecrystallized volume, and

S shape factor
G grain growth rate
R gas constant
N_0 initial number of germ nuclei per unit volume
U total energy required for a germ nuclei to become a growth nucleus (crystallite)
T_i absolute anneal temperature
t anneal time

Equation (3) is applicable to thermal annealing processes, where the time of each anneal is held constant and the anneal temperature T_i is varied for a series of M anneals.

Although G, U, S, and N_0 are known to vary with temperature,[1,3,4,8-10] the value of these parameters as a function of temperature is unknown. It will be assumed that they are constants and this should be considered when using the thermal kinetic results.

Material Samples

The samples were produced from commercially available Nickel 200 rod that has been initially cold rolled 50 percent and annealed at 631±5 K for 15 min, then cold rolled an additional 50 percent. Four samples for ultrasonic evaluation were cut from the rolled material with both sides ground and polished through 1.0 μm diamond to a mirror finish. Thirty-two specimens for metallographic, x-ray, and transmission electron microscopic analysis were also cut from the rolled stock.

Experiment

The 36 specimens (anneal batch) were initially simultaneously annealed as a group in air at 758 K for 1 hr and air cooled. Two metallography specimens were selected and permanently removed from the group for microstructural, x-ray, and transmission electron microscopic evaluation, and the four polished samples were remeasured for thickness and ultrasonic attenuation (30 to 65 MHz).[11] After ultrasonic investigation these four samples and the remaining 30 specimens were heat treated at a higher temperature. This process of specimen selection (permanent removal of two specimens) and ultrasonic evaluation of the four polished samples was repeated 16 times with the annealing temperature increased for each step and ranging from 758 to 1011 K (±5 K). The two specimens removed after each step were investigated using: (1) metallography to determine microstructural changes, (2) transmission electron microscopy to identify dislocation density variations, and (3) x-ray diffraction to determine crystalline disorder.

Microstructure

Three mutually perpendicular faces of the annealed samples were polished, etched, and photographed using standard metallographic procedures.

Three millimeter diameter, 0.38 mm thick disks were electro-discharge machined (EDM) from the annealed specimens. After the disks were hand ground to a thickness of about 0.002 cm and further electropolished to a thickness of about 800 Å, they were examined by transmission electron microscopy (TEM). At least three TEM disks were examined for each annealing temperature.

RESULTS

Ultrasonic Attenuation

The ultrasonic attenuation as a function of frequency for each of the annealing temperatures is shown in Fig. 1 and the attenuation for fixed frequency is illustrated as a function of anneal temperature in Fig. 2. While the attenuation for all temperatures increases with increasing frequency, the attenuation for constant frequencies, is observed to be a nonmonotonic function of the anneal temperature (Fig. 2). Below 800 K the attenuation (for fixed frequency) remains constant. The attenuation increases rapidly with temperature from 800 to 900 K. Although the attenuation continues to increase between 900 and 975 K it is at a much slower rate. Above 975 K the attenuation again rapidly rises with temperature. Figure 2 also demonstrates that the magnitude of the variation in attenuation over the entire anneal temperature range is more pronounced at higher frequencies.

X-Ray Analysis

The full width at half maximum (FWHM) of the (200) x-ray Bragg peak varies considerably over the annealing temperature range (Fig. 2). For temperatures below 850 K the FWHM remains relatively constant. The FWHM rapidly decreases over the range 850 to 900 K. This is an indication of increasing crystalline order with increasing anneal temperature. Temperatures above 901 K resulted in a relatively constant FWHM. The uncertainty in this measurement is relatively large as evidenced by the fluctuating FWHM at both low and high anneal temperatures.

Metallographic Results

Typical photomicrographs for the face and edge sides are shown in Figs. 3 to 8 for anneal temperatures of 758, 814, 871, 901, 940, and 1011 K (labeled T_1-T_6), respectively. As the the two perpendicular edges exhibited similar microstructure, only data for one edge is shown.

Photomicrographs of the face plane illustrate little change with annealing temperature until it equaled approximately 901 K where the unclear, worked structure remaining after lower temperature heat treatments (Figs. 3(c), 4(c), and 5(c)) is replaced by a normal grain structure (Fig. 6(c)). Higher annealing temperatures (Figs. 7(c) and 8(c)) result in little additional change except for grain growth. While examination of the face sections reveals a sharp transition in microstructure at 901 K, the edge planes show a much more gradual effect. As the annealing temperature is increased above 871 K the elongated grain structure visible in Figs. 3(b) and 4(b) is slowly replaced by a normal grain configuration (Figs. 5(b) and 6(b)) until recrystallization is nearly complete (Fig. 7(b)) and grain growth occurs (Fig. 8(b)).

Transmission Electron Microscopy

Transmission electron photomicrographs for six anneal temperatures are also shown in Figs. 3 to 8. Below 800 K TEM found only localized areas with high and low dislocation densities (Fig. 3(a)). The high and low density regions are dark and light areas, respectively, in Fig. 3. At 814 K, nucleated crystallites have started to form (Fig. 4(a)) with the nucleated crystallites varying in size and exhibiting boundaries constructed of an intertwined collection of dislocations. Figure 4 also contains regions that appear to be just forming into crystallites; these regions are believed to be germ nuclei that have just transformed into

nucleation sites. At 871 K fully developed crystallites with planar boundaries co-exist with localized regions of low and high dislocation densities (Fig. 5(a)). The 901 K anneal exhibits larger crystallites having both narrow step-like boundaries and boundaries containing a collection of oriented dislocation pile-ups (Fig. 6(a)); additionally, isolated and interconnected dislocations are present within the crystallites. After a 940 K anneal (Fig. 7(a)) the boundaries tend to have a collection of dislocations randomly attached to them, and both isolated and interconnected dislocations are present within the crystallites. At the highest anneal temperature, 1011 K, (Fig. 8(a)), only random isolated dislocations are present within the crystallites.

Correlation Between Ultrasonic Attenuation and Thermal Kinetics

Figure 9 shows the value of the key variable N (dashed-dotted curve) determined by fitting the data shown in Fig. 1 to

$$a = CF^N \tag{4}$$

The percent of recrystallization V_R/V determined by use of Eq. (3) is shown as a solid curve. Here $S = 4\pi/3$, $G = 3$ μm/hr, $U = 80$ Kcal/mole[3,8-10] and the free parameter N_o is taken to be 2×10^{18} germ nuclei/cm^3. Also shown is the percent of recrystallization, obtained from the photomicrographs,[9] for samples exhibiting about 25 to 75 percent recrystallization; larger and smaller percents could not be precisely determined by optical methods.

DISCUSSION

During the entire annealing process the attenuation at a fixed frequency either remains constant or increases with increasing anneal temperature. The dislocation density is not known quantitatively, it does, however, decrease from an extremely large to a low value as recovery and recrystallization takes place over the anneal temperature range. Therefore, dislocation damping cannot be the dominant attenuation mechanism causing the large change in attenuation observed during recrystallization. From this result it will be assumed that the grain boundary scattering is the dominant attenuation mechanism during the recrystallization process.

The onset of recrystallization is identified as the temperature at which the first germ nuclei transform into nucleated crystallites. Acoustically the onset of recrystallization begins in the temperature range 796 to 814 K where the attenuation first starts to increase (light shaded region in Fig. 10). At these anneal temperatures the small nucleated crystallites are acoustically Rayleigh scatterers yielding the large value of the exponent N (Fig. 9).

Increasing the anneal temperature produces an increasing number of nucleated crystallites and simultaneously enhances the growth rate of previously nucleated crystallites. Therefore, above 814 K there is a mixed system of Rayleigh (newly formed crystallites) and nearly stochastic (growing crystallites) scatterers. For temperatures between 814 and 975 K, the magnitude of the attenuation is expected to increase while the exponent N should decrease (see Eq. (1)). This is in agreement with Figs. 2 and 9 and is identified as the recrystallization temperature range in Fig. 10 (dark shaded region).

The completion of recrystallization is identified as the temperature at which all the germ nuclei are depleted. That is, the germ nuclei have

either transformed into nucleated crystallites or have been swallowed up by growing crystallites. The completion of recrystallization occurs between 960 and 975 K and is shown in Fig. 10 as a light shaded region.

Above 975 K pure grain growth is observed (cross-hatched region in Fig. 10). Since the grains are relatively large (approximately 50 μm diameter), for temperatures above 975 K, they (growing at rate of about 3 μm/hr) are stochastic scatterers; thus the attenuation above 975 K should increase while the exponent N should remain a constant (Eq. (1)) in agreement with Figs. 2 and 9. It should be noted here, that the attenuation in the pure grain growth region has been investigated previously[13] and found to scale with the ratio of mean grain diameter to sound wavelength indicating that dominant attenuation mechanism is grain boundary scattering.

Both the recrystallized function V_R/V and the exponent N possess similar temperature dependence (Fig. 9). The thermal kinetic results supports the attenuation data and is understood as follows. The probability of a germ nuclei transforming into a nucleated crystallite increases with increasing anneal temperature. Therefore, an initially slow recrystallization rate is followed by a rapid increase in the rate. Also, the germ nuclei transform simultaneously with the growth of previous nucleated crystallites. These growing crystallites tend to swallow up other germ nuclei so that the density of germ nuclei decreases. Therefore, there are two mechanisms that lead to a decrease in germ nuclei density. The germ nuclei become activated and transform into crystallites or they get swallowed up by growing crystallites. As a result the recrystallization rate (or the rate of formation of Rayleigh scatters) at high temperatures decreases.

A direct analogy exists between the recrystallization rate and the reaction rate observed in many chemical processes. This follows from the shape of the attenuation versus annealing temperature data. Moving from the left to the right in Fig. 10 we see an increase in the attenuation with a simultaneous increase in slope. This region is commensurate with a rapid transformation of germ nuclei to nucleated crystallites (Rayleigh scatterers). Above 901 K, the slope of the attenuation begins to decrease. This agrees with a large number of germ nuclei being swallowed up by growing crystallites (i.e., a decreased rate of Rayleigh scatterer formation). The slope of the attenuation begins to increase rapidly once more above 975 K. This is a signature that the recrystallization process has completed (i.e., germ nuclei are depleted) and only pure grain is growth present. Therefore, onset, percent, and completion of recrystallization (or onset of pure grain growth) are all identifiable from the ultrasonic attenuation as shown in Fig. 10.

The magnitude of the FWHM of a Bragg peak is dependent on several mechanisms.[2,12] When residual stresses are present the atoms are displaced from their lattice sites and this results in a broadening of the Bragg peak. It is also possible to have crystallites with similar but not identical orientation within the area covered by the x-ray beam. This will also lead to a broadening of the Bragg peak. The presence of dislocations results in high localized stresses and large displacements of atoms from their otherwise ordered crystalline structure. These large atomic displacements will lead to a broadening of the Bragg peak.

The FWHM of the diffraction peak obtains a minimum value at 901 K. This is an indication that the highest crystalline order has been obtained. However, the edge photomicrographs clearly indicate that recrystallization is incomplete (Fig. 6(b)). Bragg backscattered x-rays

probe only a few microns, so that, the FWHM diffraction data indicates that the surface of the sample has recrystallized at 901 K. This is optically supported by comparing Fig. 5(b) and (c) with Fig. 6(b) and (c).

Because TEM specimens are quite small, it is difficult to characterize the extent of any reaction without preparing and studying a large number of specimens. Even when a sufficient group is analyzed, questions can remain due to the uncertainties involved in the electrochemical thinning procedures. However, identification of small crystallites after 814 K anneal signifies that recrystallization has started at this temperature which is significantly below the minimum temperature (approximately 871 K, Fig. 5(b)) estimated from the optical metallographic evidence.

CONCLUSION

Ultrasonic attenuation was measured for cold worked Nickel 200 samples annealed at increasing temperatures. Localized dislocation density variations, crystalline order, and volume percent of recrystallized phase were examined over the annealing temperature range using transmission electron microscopy, x-ray diffraction, and metallography. The exponent of the frequency dependence of the attenuation has been found to be a key variable relating ultrasonic attenuation to the thermal kinetics of the recrystallization process. Measurement of this key variable allows for the ultrasonic determination of onset, degree, and completion of recrystallization.

X-ray, metallography, and TEM analysis individually cannot characterize the state of the recrystallization process. However, the ultrasonic attenuation, being extremely sensitive to the formation of small scatterers and having a wide dynamic range to large scatters, is able to characterize the recrystallization process.

REFERENCES

1. R.E. Reed-Hill, "Physical Metallurgy Principles," 2nd ed., Van Nostrand, New York, 1973.

2. G.E. Dieter, "Mechanical Metallurgy," McGraw-Hill, New York, 1961.

3. L.M. Clarebrough, M.E. Hargreaves, and G.W. West, Proceedings of the Royal Society, Part A, 232, 252-270 (1955).

4. J.F. Nicholas, Philosophical Magazine, 46, 87-97 (1955).

5. R. Truell, C. Elbaum, and B.B. Chick, "Ultrasonic Methods in Solid State Physics," Academic Press, NY, 1969.

6. E.P. Papadakis, Journal of the Acoustical Society of America, 37, 711-717 (1965).

7. A. Granato and K. Lucke, Journal of Applied Physics, 27, 583-593 (1956).

8. M. Avrami, Journal of Chemical Physics, 7, 1103-1112 (1939).

9. M. Avrami, Journal of Chemical Physics, 8, 212-224 (1940).

10. M. Avrami, Journal of Chemical Physics, 9, 177-184 (1941).

11. E.R. Generazio, Materials Evaluation, 43, 995-1004 (1985).

12. P. Gay, P.B. Hirsch, and A. Kelly, Acta Metallurgica, 1, 315-319 (1953).

13. E.R. Generazio, Materials Evaluation, 44, 198-202, 208 (1986).

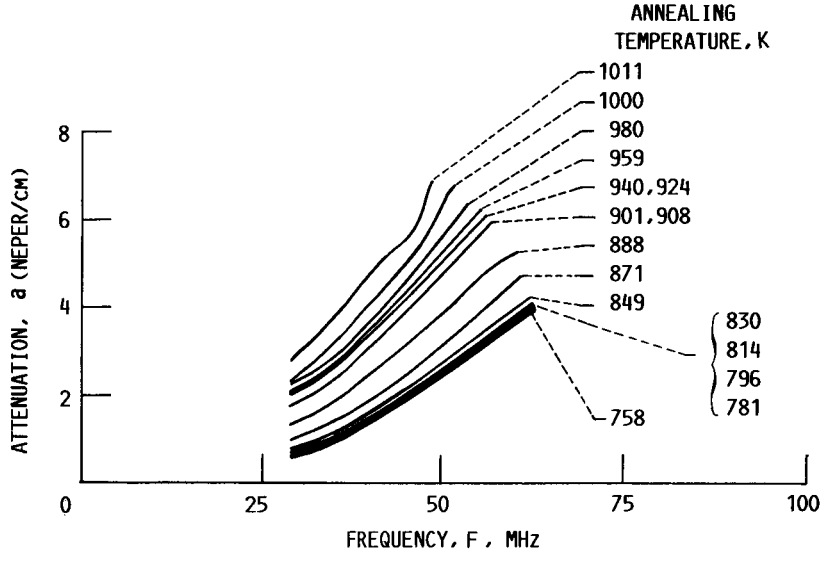

FIGURE 1. - ULTRASONIC ATTENUATION AS A FUNCTION OF FREQUENCY.

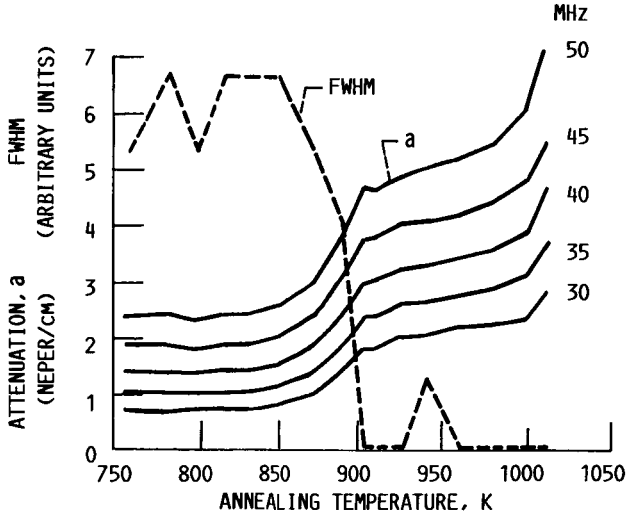

FIGURE 2.- ULTRASONIC ATTENUATION AS A FUNCTION OF ANNEAL TEMPEATURE (SOLID CURVES). THE DASH CURVE IS THE FULL WIDTH AT HALF MAXIMUM OF THE (2 0 0) X-RAY DIFFRACTION PEAK.

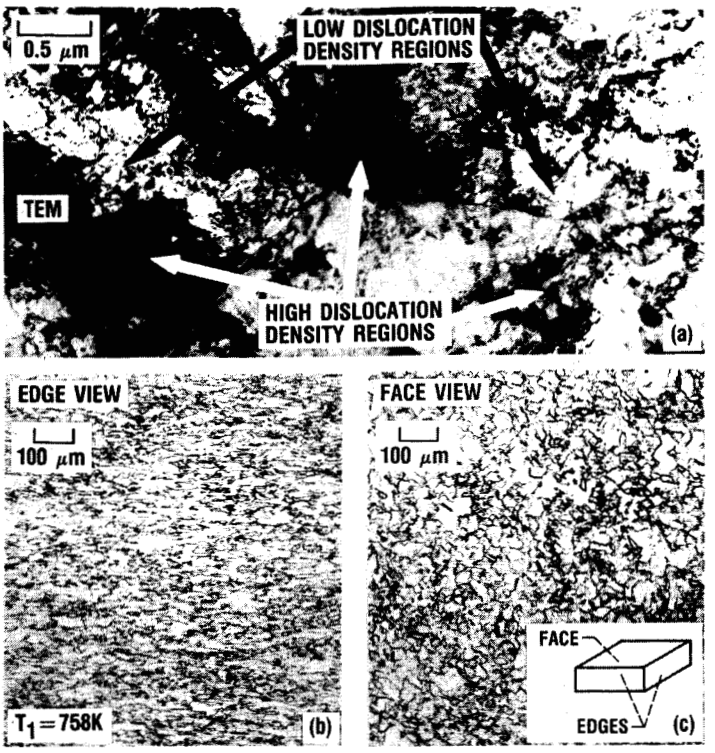

FIGURE 3. - TRANSMISSION ELECTRON MICROGRAPH, AND EDGE AND SIDE METALLOGRAPHIC VIEWS OF SAMPLE ANNEALED AT 758 K (T_1).

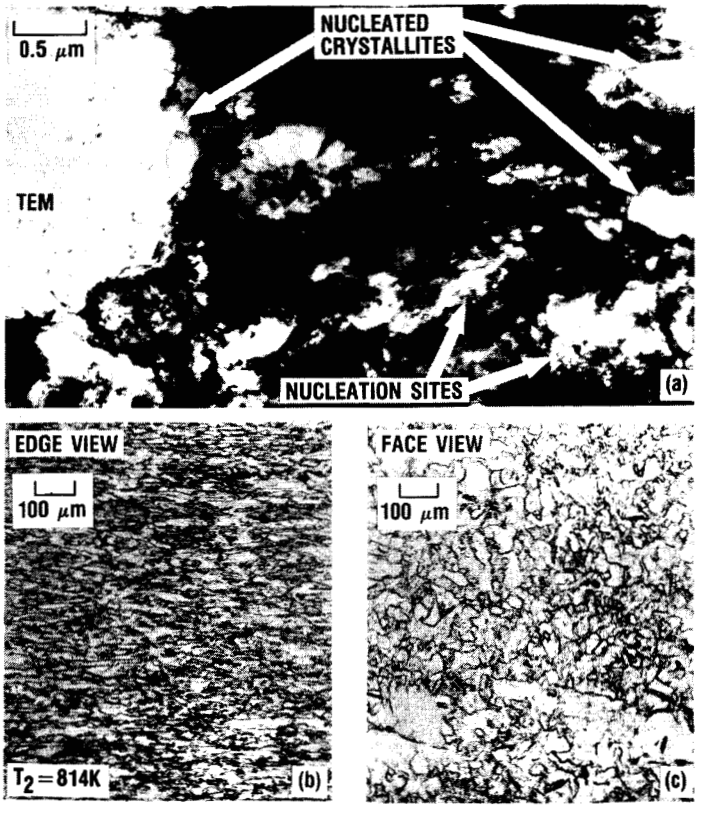

FIGURE 4. - TRANSMISSION ELECTRON MICROGRAPH, AND EDGE AND SIDE METALLOGRAPHIC VIEWS OF SAMPLE ANEALED AT 814 K (T_2).

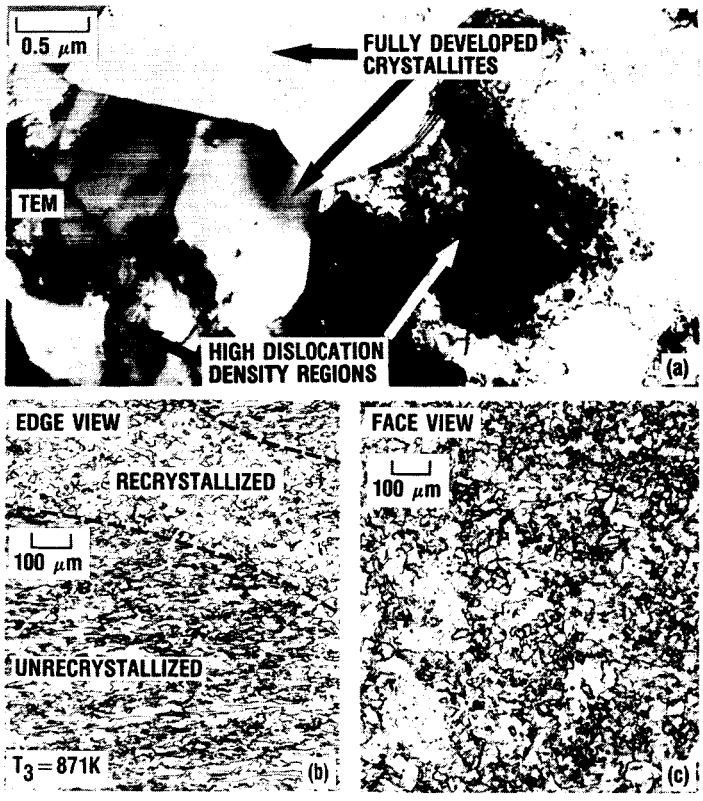

FIGURE 5. - TRANSMISSION ELECTRON MICROGRAPH, AND EDGE AND SIDE METALLOGRAPHIC VIEWS OF SAMPLE ANNEALED AT 871 K (T_3).

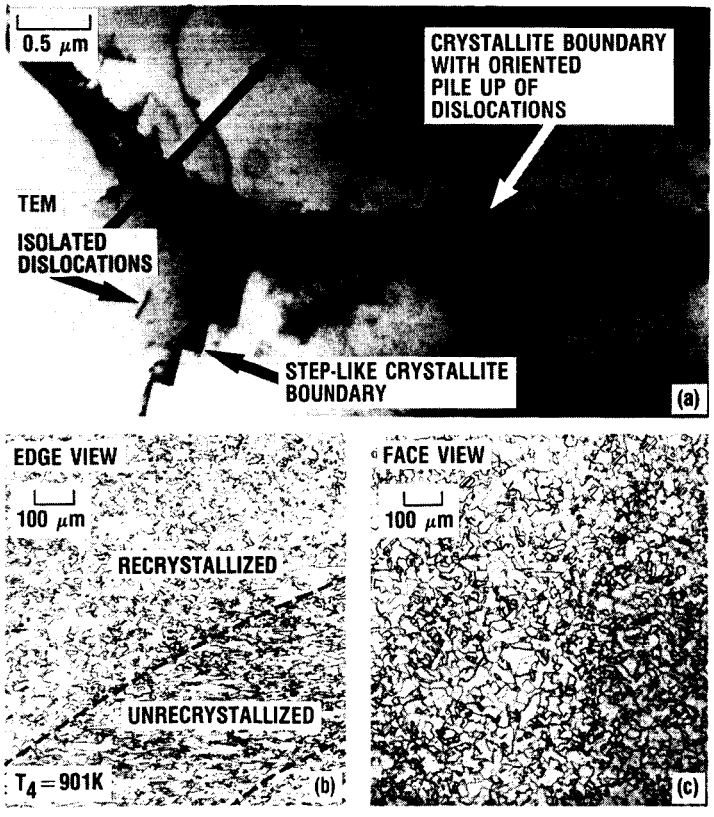

FIGURE 6. - TRANSMISSION ELECTRON MICROGRAPH, AND EDGE AND SIDE METALLOGRAPHIC VIEWS OF SAMPLE ANNEALED AT 901 K (T_4).

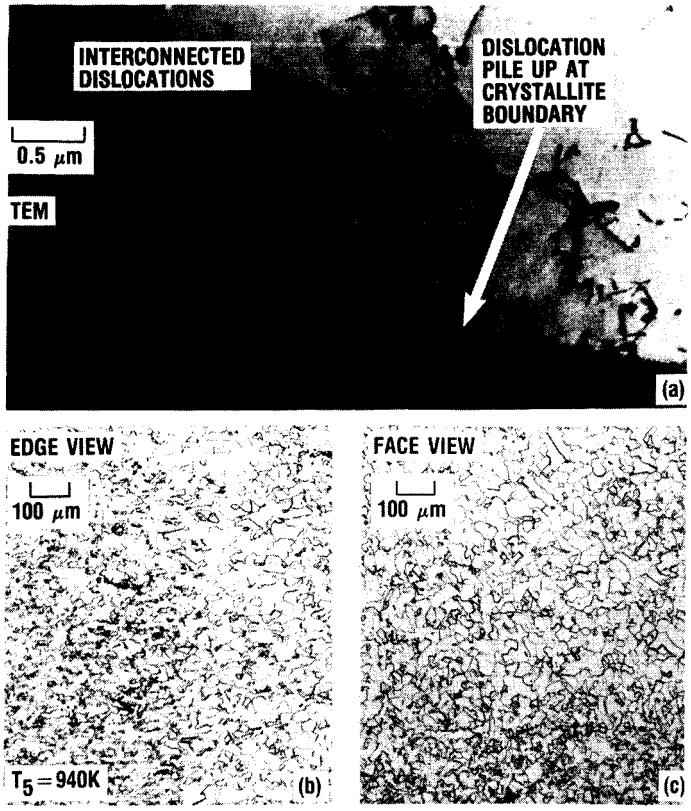

FIGURE 7. - TRANSMISSION ELECTRON MICROGRAPH, AND EDGE AND SIDE METALLOGRAPHIC VIEWS OF SAMPLE ANNEALED AT 940 K (T_5).

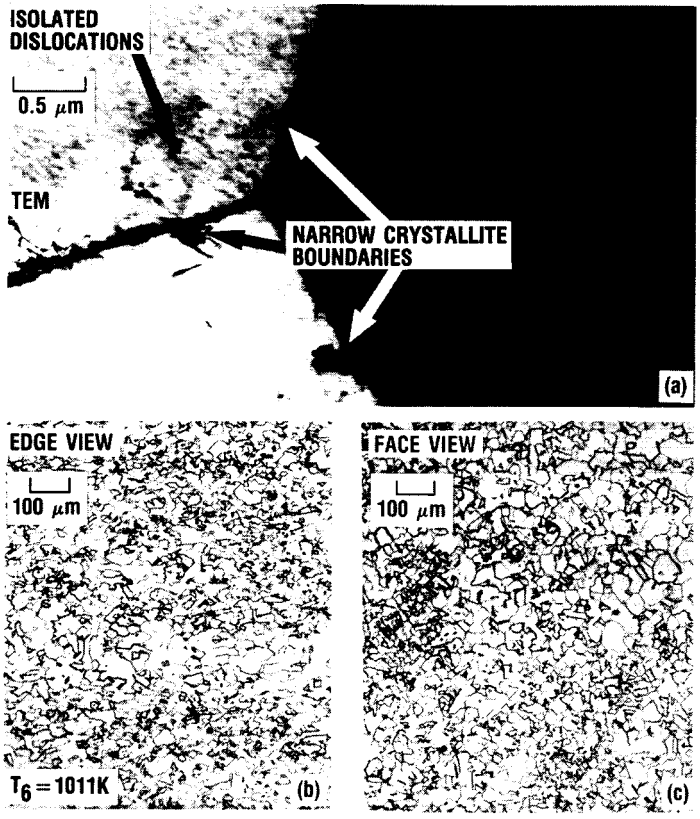

FIGURE 8. - TRANSMISSION ELECTRON MICROGRAPH, AND EDGE AND SIDE METALLOGRAPHIC VIEWS OF SAMPLE ANNEALED AT 1011 K (T_6).

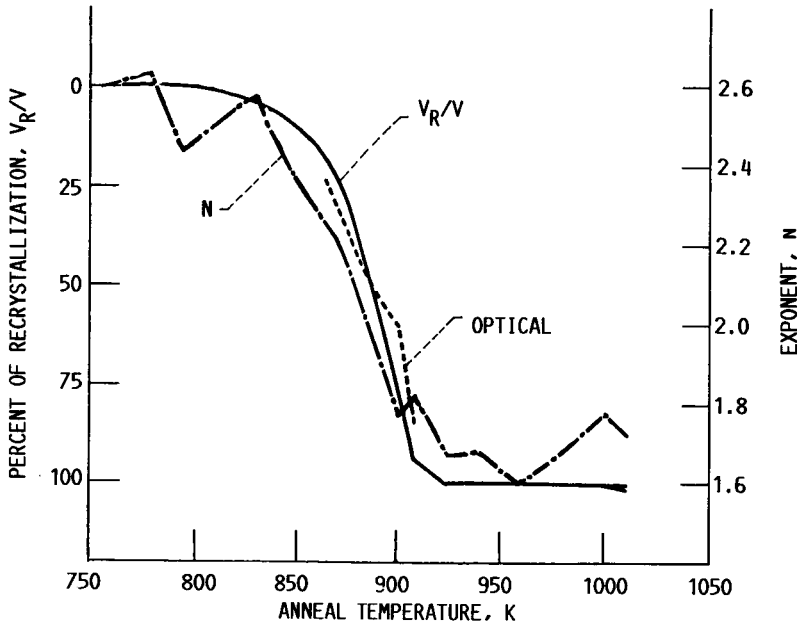

FIGURE 9.- RECRYSTALLIZATION PERCENT V_R/V DETERMINED BY USE OF EQUATION (3) (SOLID CURVE), LIGHT OPTICAL METALLOGRAPHIC TECHNIQUES (DOTTED CURVE) AND CALCULATED EXPONENT N (DASH-DOTTED CURVE) AS A FUNCTION OF ANNEALING TEMPERATURE.

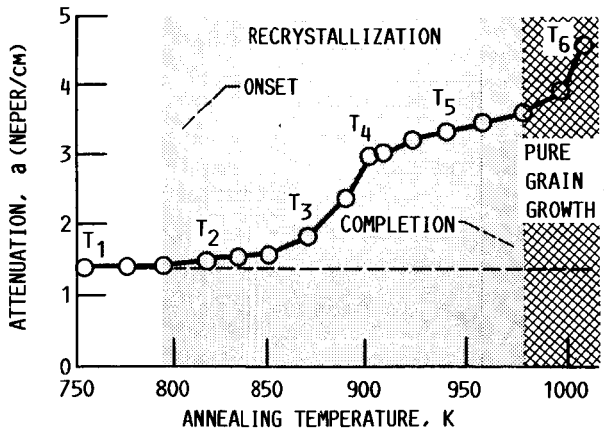

FIGURE 10.- ATTENUATION AS A FUNCTION OF ANNEALING TEMPERATURE AT 40 MHz. THE LIGHT SHADING IN THE FIGURE INDICATES ACOUSTIC IDENTIFICATION OF THE TEMPERATURE RANGES FOR ONSET AND COMPLETION OF RECRYSTALLIZATION. THE DARK SHADING INDICATES THE RECRYSTALLIZATION TEMPERATURE RANGE. THE CROSS-HATCHED REGION INDICATES THE ONSET OF PURE GRAIN GROWTH. THE TEMPERATURE LABELS T_1 TO T_6 REFER TO THE DATA SHOWN IN FIGURES 3 TO 8, RESPECTIVELY.

1. Report No.	2. Government Accession No.	3. Recipient's Catalog No.
NASA TM-88855		

4. Title and Subtitle	5. Report Date
Ultrasonic Determination of Recrystallization	
	6. Performing Organization Code: 506-43-11

7. Author(s)	8. Performing Organization Report No.
Edward R. Generazio	E-3248
	10. Work Unit No.

9. Performing Organization Name and Address	11. Contract or Grant No.
National Aeronautics and Space Administration Lewis Research Center Cleveland, Ohio 44135	
	13. Type of Report and Period Covered: Technical Memorandum
12. Sponsoring Agency Name and Address	14. Sponsoring Agency Code
National Aeronautics and Space Administration Washington, D.C. 20546	

15. Supplementary Notes

Prepared for Review of Progress in Quantitative NDE, cosponsored by the Ames Laboratory and Iowa State University, La Jolla, California, August 3-8, 1986.

16. Abstract

Ultrasonic attenuation was measured for cold worked Nickel 200 samples annealed at increasing temperatures. Localized dislocation density variations, crystalline order and volume percent of recrystallized phase were determined over the anneal temperature range using transmission electron microscopy, x-ray diffraction and metallography. The exponent of the frequency dependence of the attenuation has been found to be a key variable relating ultrasonic attenuation to the thermal kinetics of the recrystallization process. Identification of this key variable allows for the ultrasonic determination of onset, degree, and completion of recrystallization.

17. Key Words (Suggested by Author(s))	18. Distribution Statement
Ultrasonic attenuation; Nondestructive evaluation; Nondestructive testing; Grain size distribution; Recrystallization; Nucleation; Dislocations	Unclassified - unlimited STAR Category 38

19. Security Classif. (of this report)	20. Security Classif. (of this page)	21. No. of pages	22. Price*
Unclassified	Unclassified		

*For sale by the National Technical Information Service, Springfield, Virginia 22161